



Proceedings of the Sixth International Conference on
Railway Technology: Research, Development and Maintenance
Edited by: J. Pombo
Civil-Comp Conferences, Volume 7, Paper 3.16
Civil-Comp Press, Edinburgh, United Kingdom, 2024
ISSN: 2753-3239, doi: 10.4203/ccc.7.3.16
©Civil-Comp Ltd, Edinburgh, UK, 2024

Anemometer-Based Approach for Evaluating Overturning Risk Along Railway Lines

G. Crespi, S. Giappino and G. Tomasini

**Department of Mechanical Engineering, Politecnico di Milano
Italy**

Abstract

The study addresses the evaluation of overturning risk due to crosswind in rail vehicles, that is a critical concern for the safety of railway operations. In literature, studies primarily focus on high-speed trains, yet conventional trains also encounter this issue, emphasizing the need for comprehensive wind hazard assessments, applicable to all railway lines automatically. This study develops a simplified procedure for the evaluation of probabilistic distribution of wind speed and direction. By encompassing the wind climate along the railway line, this model lays the groundwork for a comprehensive risk analysis. This methodology has been applied along the Milano Novara railway line.

Keywords: crosswind, characteristic wind curves , wind analysis, anemometer, critical wind speed of overturning, low probability winds.

1 Introduction

While cross-wind effects is crucial for high-speed trains, a closer examination of lightweight railway vehicles, with commercial top speeds ranging between 160 and 200 km/h, reveals that they can also experience similar issues due to their lightness and inadequate aerodynamic shape [1]. For this reason, a new simplified method, applicable automatically to any railway line is developed in order to assess the risk for current lines and future developments.

2 Methodology

The risk analysis consists of evaluating the probability of a vehicle overturning while in motion due to crosswind action. The methodology employed at the European level for conducting this type of analysis is based on evaluating the wind speeds that cause the train to exceed 90% of the wheel axle unloading, commonly known as Characteristic Wind Curves (CWC).

The methodology for determining the risk of overturning can be outlined in three distinct phases:

1. calculation of wind speed distribution and statistical characteristics at the site;
2. calculation of CWC using, for each point, aerodynamic coefficients measured through wind tunnel tests;
3. calculation of the probability of exceeding the CWC.

2.1 Wind speed distribution at top of the rail (TOR)

For estimating atmospheric conditions at top the rail, we selected anemometers placed along the rail line of interest. This analysis will be based on three anemometers that cover the Milano-Novara Rail line as indicated below in Figure 1.

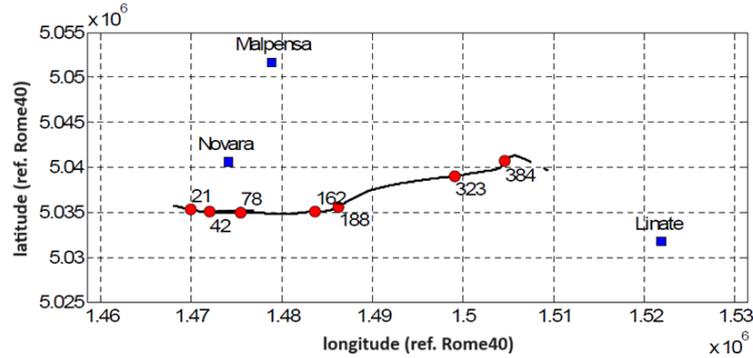


Figure 1: Map of the Milano-Novara rail line

The selected anemometers for the analysis include Malpensa, Novara, and Linate. Data is acquired from HADISD [2], which stands for "High-Quality Daily ISD." It is a dataset comprising high-quality daily observations from the Integrated Surface Database (ISD). The characteristic of 7 points analysed are depicted in table 1.

Point	Elevation	Infrastructure	azimuth
21	10.1	Embankment	96.
42	13.15	Viaduct	92.9
78	7.9	Embankment	91.
162	10.3	Viaduct	87.
188	9.1	Embankment	62.
323	10.6	Viaduct	83
384	12.8	Viaduct	31

Table 1: Milano Novara line data

The proposed methodology for assessing the wind at top of the rail is composed of 4 steps, as illustrated by the flowchart in Figure 2.

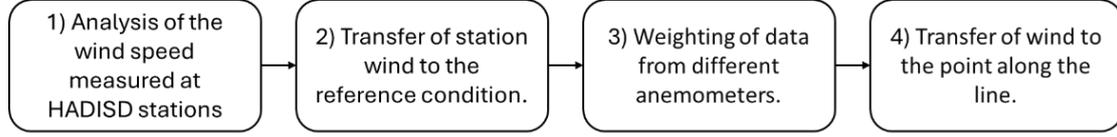


Figure 2: Block diagram of the methodology

1. The wind speed population data at each anemometer is obtained from HADISD.
2. The wind speed measurements at each station are adjusted to a reference condition with a height of $z = 10 \text{ m}$ and a roughness length of $z_0 = 0.05 \text{ m}$.
3. Since wind conditions may vary across different stations, it is essential to aggregate and weigh the data from each station to ensure an accurate assessment of wind characteristics along the railway line.
4. The reference wind speed at each station is transferred to the railway line, accounting for factors such as roughness length and infrastructure configuration.

2.1.1 Analysis of the anemometric measurements

Given the significant impact of wind directionality on the overturning phenomenon, our analysis is conducted on a directional basis, dividing the wind's origin into 12 sectors of 30 degrees each. To provide a statistical description of the wind patterns, we propose employing a hybrid Weibull distribution, as depicted in Equation 1:

$$F_v(v) = 1 + \sum_{j=1}^s A_j \exp \left[- \left(\frac{v}{c_j} \right)^{k_j} \right] (v \geq 0) \quad (1)$$

where:

- A_j is the probability, conditioned on $V > 0$, that the wind originates from the j^{th} sector.
- K_j is the shape parameter.
- C_j is the scale parameter.

The wind distribution for the anemometer with a probability of exceedance of 10^{-6} is shown in Figure 3. The highest winds come from sectors 1 and 12, meaning that the most critical points along the rail line will be the ones affected by winds from these directions.

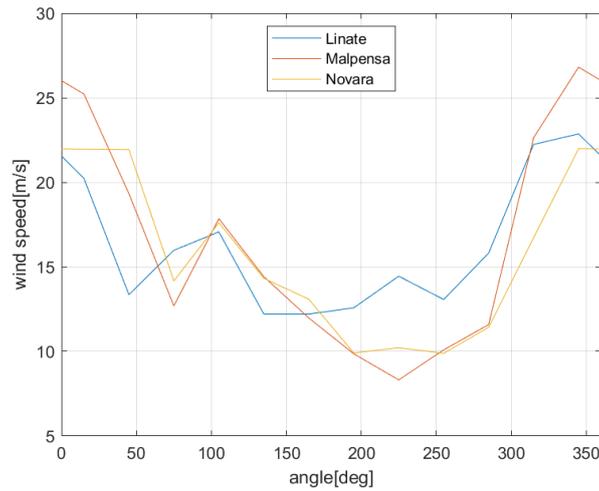


Figure 3 – Wind speed with a probability of exceedance of 10^{-6}

2.1.2 Transfer to the reference condition

The wind measured by the anemometer is scaled to the reference condition $z = 10$ m and $z_{0,ref} = 0.05$ m by using the method proposed in ESDU 82026[4]. The roughness correction should not be done punctually; the estimation of roughness takes into account a radius of 10 km through Corine Land Cover (CLC)[5], a database on land used in the European Union. In Figure 4, an example is presented for Milan Malpensa, where each sector "j" will have its associated correction factor.

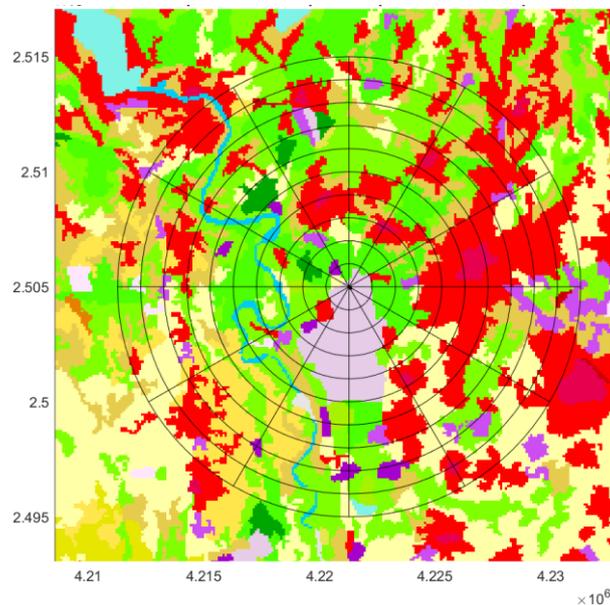


Figure 4 - CLC coverage classes for Milan Malpensa airport

For each class in this database, a roughness is assigned based in the study performed by Silva et al.[6] using the most likely value for each class. To bring the wind data to the reference, by using the equation 2:

$$V_{ref,i} = K_{s,i} V_i \quad (2)$$

where:

- $V_{ref,i}$ is the velocity measured in the anemometer “i” at reference conditions.
- $K_{s,i}$ is a roughness factor derived from the ESDU 82026[4] standard, employing the average value of each kilometer to estimate the evolution of the wind profile corresponding to each anemometer “i”.
- V_i is the measured wind speed at the anemometer “i”.

2.1.3 Weighting of Data from Different Anemometers

Wind conditions can vary between different stations, and it's necessary to weigh the data from each station to obtain an accurate assessment of wind characteristics along the line. To address this challenge, weight function models have been introduced, based on radial functions that depend solely on the distance between the anemometer station and the point along the line. This approach allows for a homogeneous and consistent transfer of data without introducing additional factors related to measurement quality, for which reliable estimates are lacking. The weight functions, ranging from 0 to 1, are designed to assign maximum weight when the distance is less than a minimum value and gradually decrease as the distance increases, ensuring a monotonic and uniform trend, according to the formula defined in Equation 3:

$$\Psi(d) = \begin{cases} 1 & d \leq d_0 \\ e^{-a(d-d_0)^2} & d > d_0 \end{cases} \quad (3)$$

In analogy to the indications provided by [7], a preliminary value of $d_0 = 20\text{km}$ has been set. It is assumed that the territorial coverage (TC) of the anemometric station within a distance r from the station itself enjoys the following property:

$$TC = \int_0^r \Psi(d) dd \quad (4)$$

It is also assumed that territorial coverage is complete when $TC \geq 0.9$. Based on these considerations, the modeling of parameter 'a' present in Equation 3 was performed considering the value of the parameter 'r' defining the coverage as 75 km, with $a = 3.55 \times 10^{-4}$.

For a point “k”, the reference speed calculated from the 3 airports ($i=1,2,3$) based on the distance from them is:

$$V_{ref,k} = \frac{\sum \Psi(d_{ki}) V_{ref,i}}{\sum \Psi(d_{ki})} \quad (5)$$

where:

- d_{ki} is the distance between point "k" on the line and airport "i".
- $V_{ref,i}$ is the reference wind speed at the airport “i”.

The weighting factor for the different points are presented in table 2.

	21	42	78	1621	188	323	384
Linate	0.257	0.266	0.28	0.307	0.314	0.334	0.34
Malpensa	0.371	0.367	0.36	0.346	0.343	0.334	0.333
Novara	0.371	0.367	0.36	0.346	0.343	0.333	0.327

Table 2: Milano Novara line data

2.1.4 Transfer of the wind to the rail line

The wind speed along the line is calculated for 12 angular sectors, each of 30 degrees, for the different isoquants of interest ranging from 10^{-4} to 10^{-10} . To estimate the wind along the line, synthetic coefficients are employed, following Equation 6:

$$V_{WL,k} = V_{REF,k} K_S K_I \quad (6)$$

where:

- K_S is a coefficient used to adjust from the reference conditions to the actual roughness length and height. For embankments, the height is set at 4m above the flat ground, and for viaducts, it is 2m above the top of the rail.
- K_I is a correction coefficient that accounts the type of infrastructure, equal to 1 for the viaducts and for the embankments is the equation 7.

Railway embankments, similar to natural topographies, create a phenomenon known as speed-up, characterized by the acceleration of the incident wind flow. This phenomenon is complex due to various parameters, including the heights of the embankment above and below the wind (H_U and H_D), the width, the slope ϕ , the position W relative to the cross-section, and the evaluation altitude.

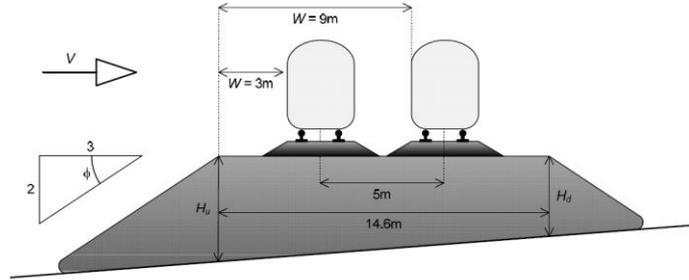


Figure 5 - Schematic representation of a generic railway embankment

$$K_I = \sqrt{(\cos \alpha)^2 + (C_E \sin \alpha)^2} \quad (7)$$

where:

- α is the absolute angle of the wind speed (Figure 8b)

Previous studies have shown that various heights of the embankment above and below the wind do not have a significant impact on the wind speed. Furthermore, it has been suggested that considering the train on the windward side ($W = 3$ m) is a conservative choice. In these conditions, C_E [8] is calculated using the following expression:

$$C_E = 0,94[1,63 H_U + 10]^{1/5} - 0,49 \quad (8)$$

where:

- H_U is the height of the embankment as show in Figure 5.

2.2 CWC

The CWC represent the wind speeds at which the train reaches the overturning limit value. Conventionally, as an index, the 'wheel unloading' is adopted, which is the ratio between the variation in vertical load on the wheel compared to the static case and the vertical load under stationary vehicle conditions. The approach used for calculating CWC described in the TSI regulations [3] is the deterministic 'Chinese Hat' method, which reproduces an ideal wind gust and calculates the vehicle's dynamic response to the aerodynamic forces generated by the gust.

This procedure is based on defining a specific wind speed temporal profile to use as input for dynamic vehicle simulation. This wind speed input consists of an equivalent wind gust ('Chinese Hat') that approximates a stochastic process near a local maximum (Figure 6). Once the wind speed temporal profile is known, aerodynamic loads are evaluated using static aerodynamic coefficients measured on scaled models of the vehicle during wind tunnel tests.

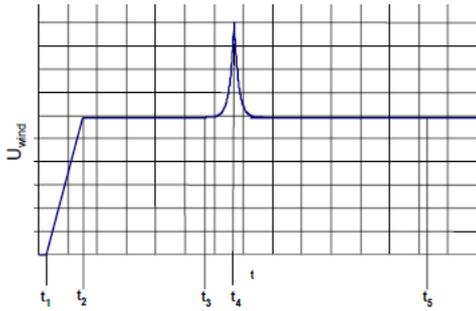


Figure 6a - Example of time-history generated with deterministic TSI method

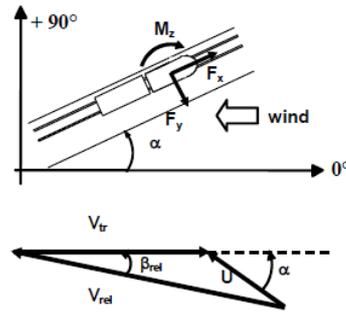


Figure 6b - Reference system adopted for the calculation of forces and velocity vectors diagram.

TSI provides detailed guidelines for creating the gust profile, starting from wind characteristics provided: the relationship between the maximum wind speed U_{max} and the corresponding mean value U_{mean} is calculated based on the normalized gust amplitude. Once the wind speed temporal profile is defined, it must be filtered with a spatial filter of dimensions equal to the vehicle length: this step accounts for the effect of wind spatial distribution on a vehicle with specific dimensions.

The five force and moment components (F_y , F_z , M_x , M_y , and M_z) are calculated using equation 9 and equation 10:

$$\left. \begin{aligned} F_i(t) &= \frac{1}{2} \rho A C_{Fi}(\beta_{rel}(t)) V_{rel}^2(t) & i \in \{y, z\} \\ M_j(t) &= \frac{1}{2} \rho A H C_{Mj}(\beta_{rel}(t)) V_{rel}^2(t) & j \in \{x, y, z\} \end{aligned} \right\} \quad (9)$$

where C_{Fi} and C_{Mj} are the aerodynamic coefficients, ρ is the air density, A is the reference area, H is the reference length of the vehicle, and where:

$$V_{rel}(t) = \sqrt{(V_{tr} + U(t) \cos \alpha)^2 + (U(t) \sin \alpha)^2}$$

$$\beta_{rel}(t) = \text{atan} \left(\frac{U(t) \sin \alpha}{V_{tr} + U(t) \cos \alpha} \right) \quad (10)$$

In equation 10, $U(t)$ represents the undisturbed wind speed. Regarding the average aerodynamic coefficients, according to TSI regulations, they must be identified through wind tunnel tests conducted with the STBR (Single Track Ballast and Rail) reference scenario.

The results of the CWC are presented in Figure 7. The most critical angles with respect to crosswind are those characterized by the lower wind speed. We can divide them into three groups based on the azimuth of the rail line. All points, except for 188 and 384, have an azimuth near 90 degrees. Therefore, the most critical angles of the wind come from the north and south directions, with point 21 having a minimum speed of 20 m/s. Point 188 has an azimuth of 60 degrees, so the critical angles are 150 and 330 degrees, with a minimum speed of 19 m/s. Point 384 is the least critical, with a minimum speed of 23 m/s at 120 and 300 degrees.

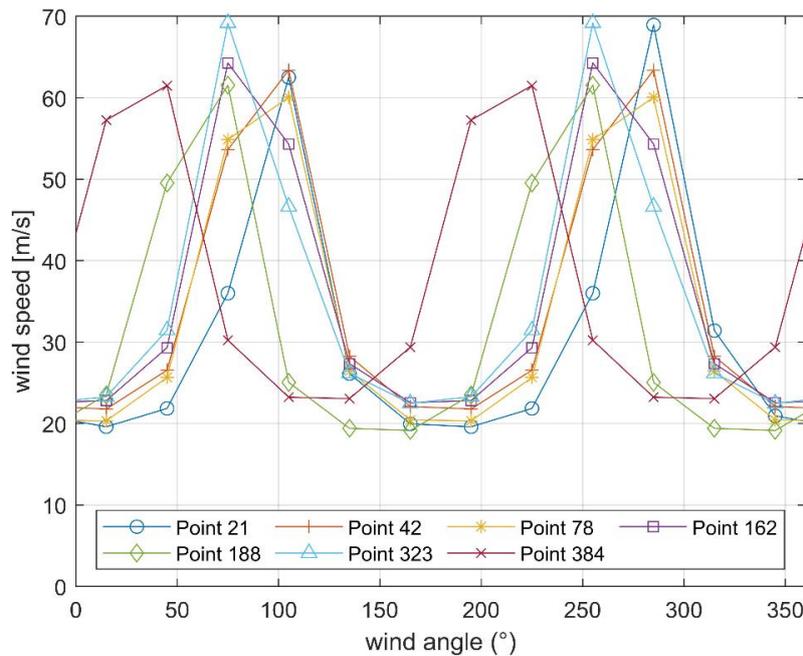


Figure 7 – CWC for the studied points along the Milano-Novara rail line.

2.3 Overturning risk

The weather study provides, for each analysed case, the cumulative probability functions (p_w) of wind speed (mean value), for discrete probability values (iso-quantiles) $p_w = [10^{-2} \ 10^{-3} \ 10^{-4} \ 10^{-5} \ 10^{-6} \ 10^{-7} \ 10^{-8} \ 10^{-9} \ 10^{-10}]$.

Wind intensity values with assigned probability of non-exceedance have been calculated directionally, i.e., for wind coming from 12 discrete angular sectors of 30° each. These functions represent the probability of the wind arriving from that sector s ($s=1:12$, Table 3) at that speed.

s	1	2	3	4	5	6	7	8	9	10	11	12
β_w	15°	45°	75°	105°	135°	165°	195°	225°	255°	285°	315°	345°

Table 3 - Angular sectors considered in the meteorological analysis

The CWC represents the probability that, for a given wind speed from a particular direction, the safety index (wheel unloading) exceeds the 90% threshold. The probability of exceeding the CWC for the i -th point of the line P_i is the integral of the exceedance probability evaluated over all "i" angular sectors p_j . In other words, since the latter is evaluated for a discrete number of angular sectors, it is the sum of the combined probability calculated for each angular sector at the i -th point.

$$P_i = \sum_{s=1}^{12} p_j \quad (11)$$

3 Results

The results for the wind transfer coefficients from the anemometric stations to the reference conditions are presented in Table 4 for each sector "j". The higher the coefficients, the greater the urbanization near the airport. That's why Linate has the highest coefficients, due to its proximity to the city center.

s	1	2	3	4	5	6	7	8	9	10	11	12
$K_{s,1}$	1.10	1.13	1.07	1.21	1.30	1.29	1.14	1.04	1.05	1.12	1.13	1.09
$K_{s,2}$	0.94	1.10	1.12	1.08	1.01	1.09	1.16	1.10	1.08	1.07	1.02	1.00
$K_{s,3}$	1.03	1.13	1.10	1.09	1.12	1.08	1.01	1.02	0.99	1.02	1.02	1.04

Table 4: Transfer coefficients from the anemometers to the reference condition.

where:

- $i=1$ is Linate.
- $i=2$ is Malpensa.
- $i=3$ is Novara.

In Figure 8 the transfer coefficient from the reference conditions to the airport are presented. The point 21, 42 and 323 show the highest coefficients in correspondence

with the minimum of the CWC showed in Figure 7. The point 384 show a big transfer coefficient at 225°

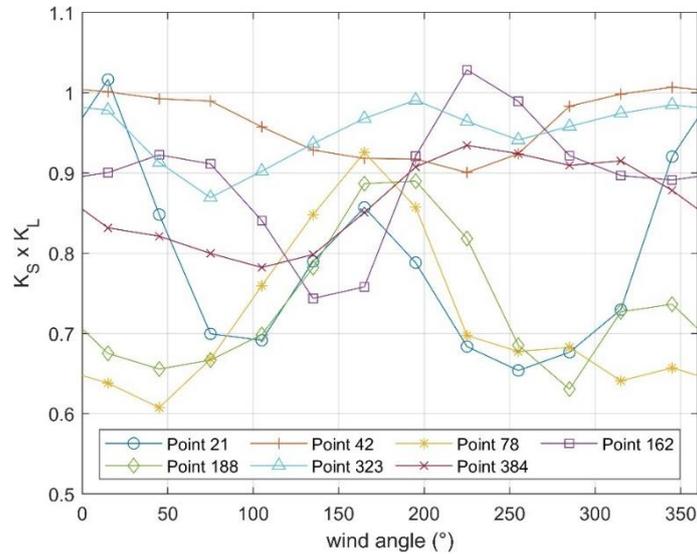


Figure 8 – Transfer coefficients for the points studied along the rail line.

Figure 9 shows the CWC and the isoquants for point 21 and 42. The dashed line shows the probability of exceeding a certain wind speed, while the continuous red line shows the CWC of the train at that point on the track. With the azimuth of the track around 90 degrees, the most critical conditions arise near 0 and 180 degrees.

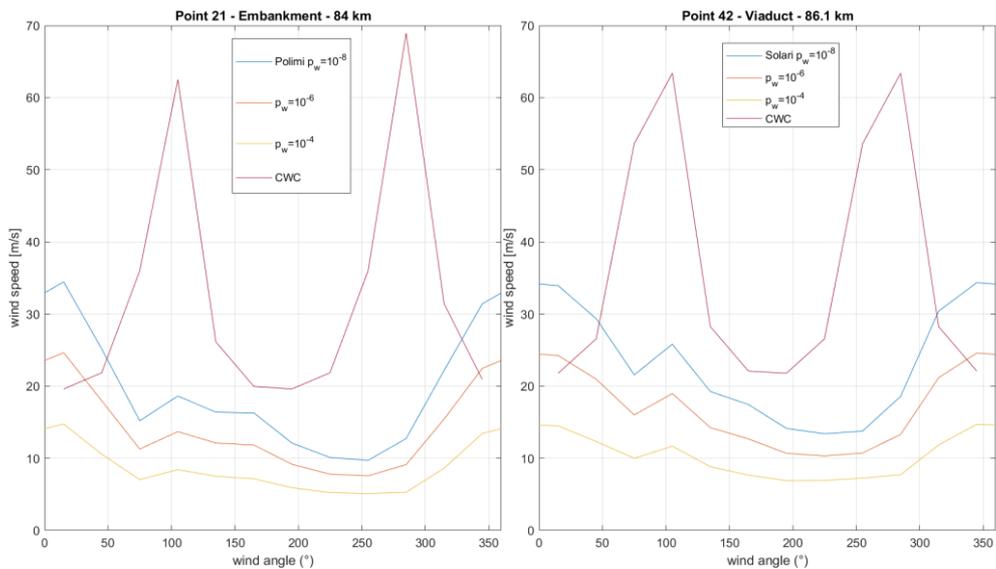


Figure 9 – Wind probability for several isoquants and CWC at point 21 and 42

The overturning probability of a point is calculated by summing the probability of overturning for each sector. In Figure 10 it can be seen a summary of the exceedance probability for all the rail line where the most critical points are point 21 and 42.

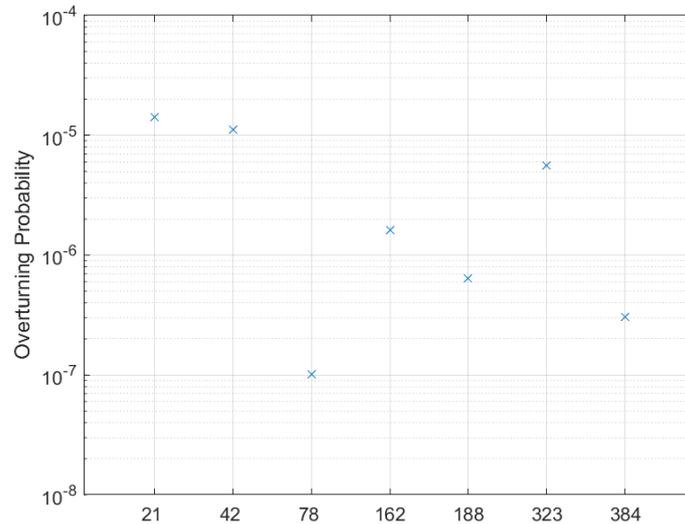


Figure 10 – Overturning probability for the point along the Milano – Novara rail line

4 Conclusions and Contributions

In this research, a new simplified methodology for the evaluation of the overturning risk along a railway line has been setup and applied to the Milano Novara rail line. This procedure allows to assess the most critical points along the line, accounting for different parameters i.e. :

- the atmospheric wind in the line of interest starting from anemometers;
- the highly directional component of the overturning risk, asses in 12 different sectors;
- the influence of the infrastructure;
- the roughness near to the rail line that has a considerable impact on how the atmospheric boundary layer develops.

Acknowledgements

The study illustrated in this paper was carried out on behalf of Rete Ferroviaria Italiana (RFI), and it was financially supported by this company.

References

- [1] S. Giappino, D. Rocchi, P. Schito, G. Tomasini. (2016). Cross wind and rollover risk on lightweight railway vehicles. *Journal of Wind Engineering and Industrial Aerodynamics*. 153. 106-112. 10.1016/j.jweia.2016.03.013.
- [2] Dunn, R. J. H., Willett, K. M., Parker, D. E., and Mitchell, L. (2016) Expanding HadISD: quality-controlled, sub-daily station data from 1931, *Geosci. Instrum. Method. Data Syst.*, 5, 473491, <https://doi.org/10.5194/gi-5-473-2016>

- [3] TSI HS LOC&PASS 2014/1302/CE - European Rail Agency. Technical Specification for Interoperability – Rolling Stock subsystem, 96/48/EC
- [4] ESDU 82026. "Strong winds in the atmospheric boundary layer. Part 1: hourly-mean wind speeds."
- [5] CORINE Land Cover 2018 (raster 100 m), Europe, 6-yearly - version 2020_20u1, May 2020
- [6] Silva, J., Ribeiro, C., Guedes, R., Rua, M.-C., & Ulrich, F. (2007). Roughness length classification of Corine Land Cover classes. In Proceedings of EWEC 2007
- [7] World Meteorological Organisation, 1996, Guide to meteorological instruments and methods of observations, WMO-No. 8, 6th edition.
- [8] Baker, C.J., (1985). The determination of topographical exposure factors for railway embankments, J. Wind Engng. Ind. Aerod., 21 (1), 89-99.